

Approaching energy quantum limit detection of microwave photons with Josephson Junctions

Y. Q. Chai,¹ S. N. Wang,¹ P. H. OuYang,¹ and L. F. Wei ^{*1}

¹*Information Quantum Technology Laboratory, International Cooperation Research Center of China Communication and Sensor Networks for Modern Transportation, School of Information Science and Technology, Southwest Jiaotong University, Chengdu 610031, China*

(Dated: November 1, 2024)

Single-photon detection is an energy quantum limit detection (EQLD) of a significantly weak electromagnetic wave. Given the sensitivity of the conventional electromagnetic induction microwave receiver working at room-temperature is very limited, due to the significantly strong thermal noise, here we analyze the possibility of approaching the EQLD of the weak microwave signal by using a current-biased Josephson Junction (CBIJ) detector. By numerically simulating the dynamics for the phase particle of the CBIJ, we propose an approach to describe the discriminability between the probabilistically escaped events of the phase particle with and without the microwave current driving, by measuring the minimum d_{KC} -index. We predicate that, the experimentally demonstrated CBIJ detectors possess the ability to resolve about a dozen photons. The feasibility of the desired EQLD of microwave signal by using the CBIJ detector is also discussed.

I. INTRODUCTION

Microwave receiver is a system to sensitively detect the microwave signal in noisy environments. It is well-known that one of the biggest obstacles to improve the detection sensitivity is the thermal noise; e.g., at 290 K room temperature, the sensitivity is limited as $4 \times 10^{-18} \text{ W}/\sqrt{\text{Hz}}$ [1], which is far from the energy quantum limit detection (EQLD) at the single-photon level [2–8]. Although the sensitivity can be improved by developing various techniques, such as phase lock amplifications [9], multi-branch receptions [10], outlier detection [11], and digital-to-analog conversions [12], etc., the reachable sensitivity is still very limited [13–15]. Therefore, the development of the higher sensitivity microwave receiver is still a great challenge, specifically for solid-state quantum computing [16–19], microwave quantum sensing [20], and also for the sensitive detection of either gravitational waves in GHz band [21, 22] or the axion dark matters with μeV -order masses [23, 24], etc.

Physically, the energy of a microwave photon is at $\sim 10^{-24} \text{ J}$ level, which is 4–5 orders of magnitude lower than the energy of a single photon at the optical band. This implies that the microwave single-photon detector should work in the mK-order temperature regime for the effectively suppressing the relevant thermal noise. For example, if a superconducting microwave receiver is worked at 10 mK, its realizable detection sensitivity could be estimated as $\sim 10^{-23} \text{ W}/\sqrt{\text{Hz}}$ [1], which is theoretically improved the sensitivity by 5–6 orders of magnitude relative to a room-temperature microwave receiver. Therefore, various cryogenic superconducting devices could be served as the natural candidates to implement the sensitive detection of the weak microwave signal for approaching the corresponding EQLD.

Until now, a series of approaches have been really demonstrated to implement the desired microwave single-photon detection, i.e., at EQLD level. The first one is called resonant

detection, which is usually implemented by probing the microwave single-photon induced resonant quantum transition, between the levels of the artificial atom [25–27]. The second one is achieved by using the low-noise Josephson parametric amplifier [28, 29] to amplify the single-photon signal for the later detection. However, what the former realization is the narrow band detection, as its detection efficiency is basically determined by the resonantly or near-resonantly excited probabilities of the ground-state artificial atoms, driven by the microwave photon. While, the detection sensitivity demonstrated by the latter one is very limited, due to the influence from the addition noise of the driving source [30]. Therefore, fast, highly efficient, and highly sensitive detection of the microwave single photons are still a great challenge for the desirable microwave quantum information processing (such as the superconducting quantum computation [31, 32], microwave quantum radar and the microwave quantum sensing [33]), and also the significantly weak microwave response detections of the μeV -mass axion dark matter [23, 24] and the microwave band gravitational waves [21], in the stationary strong magnetic fields.

Focusing on such an urgent requirement, in the present work we investigate the possibility of the fast and sensitive detection of microwave photons, specifically with the experimental current-biased Josephson Junction device. Here, the CBIJ is a highly quality Josephson junction biased by a dc-current, whose amplitude is slightly less than its critical current, and the detected weak microwave signal is treated as a modified biased current. Based on the usual RCSJ model [34, 35] with the noise current driving, we numerically simulate the dynamics of the phase particle driven by the driven microwave current signal, for describing the switching behavior of the junction being transited from the zero-voltage state into the finite voltage one [36–39]. By comparing the switching behaviors of the CBIJ with and without the driven microwave signal, we quantify its detectability by the measured Kumar Carroll (KC) index [40, 41], effectively.

The paper is organized as follows. In Sec. II, based on the usual RCSJ model, we numerically solve the dynamics for a phase particle driven by thermal noise, and then discuss how to implement the weak microwave signal detection by probing

*Corresponding author. lfwei@swjtu.edu.cn

the escape effect of the phase particle. A so-called minimum $\min[d_{KC}]$ index is introduced to characterize the detectability of the junction being switched from the zero-voltage state into the finite voltage state. In Sec. III, we specifically investigate how to detect microwave current pulse signals containing N photons applied to the CBJJ. With the demonstrated CBJJs, the minimum number of the detectable microwave photons are estimated. In Sec. IV, we summarize our results and discuss the possibility of using the CBJJ device to implement the EQLD of a single microwave photon.

II. DYNAMICAL SIMULATION FOR THE ESCAPES OF A DRIVEN PHASE PARTICLE

A single Josephson Junction (JJ) without current bias consists simply of two superconducting electrodes sandwiched between a layer of thin insulator, and obeys the following Josephson relation [42]

$$I_J = I_0 \sin(\varphi), \quad V = \frac{\hbar}{2e} \frac{d\varphi}{dt} \quad (1)$$

where I_J , φ and V are the Josephson current, macroscopic phase and voltage of the junction, respectively. I_0 , \hbar , and $2e$ are the critical currents (denoting the maximum Cooper-pair tunneling current through the junction), the reduced Planck constant and the Cooper-pair charge, respectively. Under a dc-current I_b bias, the device can be described effectively by a capacitive-resistive shunt model (RCSJ model) [34, 35], shown in Fig. 1(a), and thus

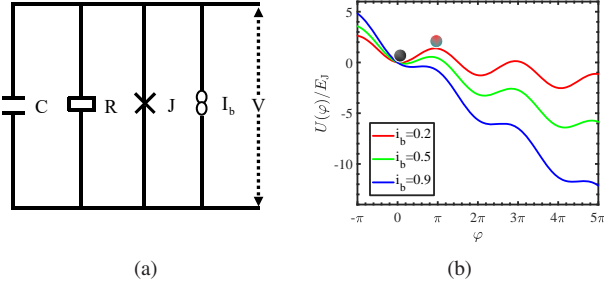


FIG. 1: A CBJJ device can be described by: (a) A RCSJ equivalent circuit, where V is the voltage across JJ, C , R , and I_b denote the capacitance, and resistance of the Junction J, respectively. (b) A macroscopic phase particle moving in the washboard potentials, which has been normalized to the Josephson energy $E_J = \hbar I_0 / 2e$, for different biased currents. Here, the red, green, and blue solid lines indicate the washboard potentials generated by different biased currents. The ball represents the states of the CBJJ; the black- and cyan-red balls refer to zero-voltage and the finite voltage states of the CBJJ, respectively.

$$\begin{cases} I_C + I_R + I_J = I_b, \\ \frac{\hbar C}{2e} \frac{d^2\varphi}{dt^2} + \frac{\hbar}{2eR} \frac{d\varphi}{dt} + I_0 \sin(\varphi) = I_b, \end{cases} \quad (2)$$

in the absence of noise. Here, I_C and I_R represent the currents flowing through the capacitor and resistor, respectively. Formally, such a current-biased Josephson junction (CBJJ) device can be described as a “phase particle” of “mass” $m = C(\hbar/2e)^2$ moving in a so-called the washboard potential [43],

$$U(\varphi) = E_J [1 - \cos(\varphi) - i_b \varphi], \quad i_b < 1, \quad (3)$$

where $i_b = I_b/I_0$, and shown schematically in Fig. 1(b). The height of the potential barrier is [44]

$$\Delta U(\varphi) = 2E_J \left[\sqrt{1 - i_b^2} - i_b \arccos(i_b) \right]. \quad (4)$$

Phonemically, depending on if the phase of the particle is less or larger than the critical phase φ^* , i.e., the trapped particle is at its highest energy value, the CBJJ is in either the superconducting state with $V = 0$ (i.e., the color of the “phase particle” is black) or the finite voltage state with $V \neq 0$ (i.e., the color of the “phase particle” is cyan-red). Correspondingly, the current flowing through the JJ satisfies the condition; either $i_b > 1$, or $i_b < 1$. Therefore, for a CBJJ with a dc-current i_b , the slowly added microwave current δi increases the energy of the phase particle consequently, until it escapes finally from the potential well. This means that by probing the induced finite voltage state transited from the zero-voltage, i.e., the color of the particle is transited from black to cyan-red, the applied microwave current with the relevant energy can be detected.

A. Dynamics of the coherently driven phase particle in absence of noise and the voltage-state switch

Besides the dc-current bias, we first treat simply the applied microwave as an additional weak coherent current,

$$I_s = I_{MW} \sin(\omega_s t), \quad (5)$$

with ω_s and I_{MW} are the frequency and amplitude of the applied microwave current, respectively. As a consequence, the RCSJ equation shown in Eq. (2) can be modified as

$$\frac{d^2\varphi}{d\tau^2} + \beta \frac{d\varphi}{d\tau} + \sin(\varphi) = i_b + i_s, \quad (6)$$

where $\beta = 1/RC\omega_J$, $i_s = I_s/I_0$ and $i_b = I_b/I_0$ are the damping parameter, the normalized bias current, and the weak signal current, respectively. $\omega_J = \sqrt{2eI_0/\hbar C}$ is the plasma frequency of the JJ [43]. Physically, without such a coherent microwave current, the phase particle damps oscillates in the washboard potential, whose height is defined by the normalized biased dc-current i_b . Due to the applied microwave current i_s , the barrier height of the washboard potential oscillates also with the frequency of ω_s . This implies that the phase particle possesses certain probabilities to be escaped out of the well. It is an observed fact that the phase particle is more likely to escape from the potential well if the frequency of the microwave signal is near resonance with JJ’s Plasma fre-

quency. However, it is noted that the Plasma frequency of CBJJ is modulated as $\omega_J^* = (1 - i_b^2)^{1/4} \omega_J$, due to the bias current i_b . This makes the transition between the CBJJ voltage states extremely sensitive to the microwave signal, if the $\omega_s \cong \omega_J^*$.

To numerically simulate the escape behavior of the driven phase particle, we introduce a critical phase value φ^* for the phase variable $\varphi(\tau)$, $\tau = \omega_J t$ and define $V = 0$ for $\varphi \leq \varphi^*$ and $V \neq 0$ for $\varphi > \varphi^*$. By randomly-selected initial phase $\varphi(0) = [-0.1, 0.1]$, the initial voltage $V(0) = d\varphi/d\tau|_{\tau=0} = 0$ and also the critical phase $\varphi^* = \pi$, one can numerically solve Eq. (6) to simulate the possible escape events of the phase particle; once the phase variable $\varphi(\tau)$ is evolved to the time τ^* with $\varphi(\tau^*) > \pi$, we get an event of

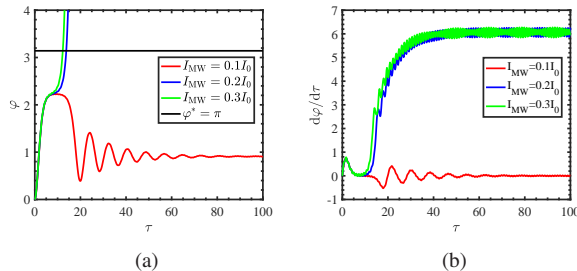


FIG. 2: The simulated phase dynamics (a) and voltage changes (b), by numerically solving Eq. (6). Here, the length of the time step is set as $\delta t = 0.0001$ and the JJ parameters are set as [45]: $I_0 = 8.586 \mu\text{A}$, $R = 29 \Omega$, and $C = 2700 \text{ fF}$, respectively. The biased dc-current and the frequency of the microwave signal are set as $i_b = 0.789$ and $\omega_s/2\pi \approx 12.25 \text{ GHz}$, respectively.

the JJ being switched from the superconducting state into the finite voltage state with $\dot{\varphi}(\tau) \neq 0$, and then run another simulation. Repeating such a numerical simulation multiple times. Fig. 2 shows these switching behaviors for signals with different amplitudes, wherein the red lines refer to that the JJ still stays at the zero-voltage state and the green and blue lines indicate that the JJ has been switched into the finite voltage states with $\varphi > \varphi^*$ and $\dot{\varphi}(\tau) \neq 0$. Therefore, weak microwave signals can be detected by using the CBJJ devices; the larger the bias dc-current i_b , which yields the value of i_b is closer to 1, and thus the smaller amplitude I_{MW} of the signal can be detected, for the given JJ parameters. The stronger the microwave signal corresponds to the larger the measurable voltage. Ideally, an arbitrarily weak microwave signal can be detected, if the bias current i_b flowing through the CBJJ is regulated such that i_b is infinitely close to 1. Obviously, this is impossible, as any actual device is necessarily noisy.

B. Detectability of the escape events of coherently driven phase particle in the presence of noise: the Kumar-Caroll index

In practice, the switching of the JJ voltage state is due to not only the microwave weak signal, which is expected to be detected, but also various practically-existing noises, typically such as the thermal- [46] and macroscopic quantum tunneling

fluctuations [47–49]. Below, we investigate specifically how the applied coherent microwave signal yields the escape of the phase particle from the potential well, specifically in the presence of thermal noise. To this end, we solve the following Langevin equation

$$\frac{d^2\varphi}{d\tau^2} + \beta \frac{d\varphi}{d\tau} + \sin(\varphi) = i_b + i_n, \quad (7)$$

instead of Eq. (6). Above, $i_n = I_n/I_0$ is the normalized noise current, which satisfies the following statistical distribution feature [50]

$$\begin{aligned} \langle i_n \rangle &= 0, \\ \langle i_n(\tau) i_n(\tau') \rangle &= 4 \int_{-\infty}^{\infty} df \frac{hf\omega_J \exp(i2\pi f(\tau - \tau'))}{RI_0^2(\exp(hf/k_B T) - 1)}, \end{aligned} \quad (8)$$

for the thermal noise described by Planck blackbody radiation law. The parentheses $\langle x \rangle$ denote the statistical average of the noise current, f , T , h , and k_B are radiation frequency, temperature, Planck-, and Boltzmann constants, respectively. Note that, here the thermal noise described by the standard Planck spectrum (8), rather than its high-temperature limit (i.e., the Nyquist noise: $\langle i_n(\tau) i_n(\tau') \rangle = 4k_B T/R$) used typically in Refs. [38, 46, 51, 52], as the present device works practically at the ultra-low temperature regime wherein the usual high-temperature approximation $k_B T \gg hf$ is not satisfied.

We use the Eulerian algorithm [53, 54] to solve the above Langevin equation numerically to simulate the kinetic behavior of the “phase particle”. For simplicity, the amplitude of the noise current is treated specifically as

$$\Delta i_n = \sqrt{\langle i_n(\tau) i_n(\tau') \rangle \delta t} N(0, 1), \quad (9)$$

where δt is the time step, and $N(0, 1)$ denotes a Gaussian-distributed random number generated by using the Box-Müller method [55, 56]. According to Eqs. (3) and (4), we know that the proper selection of bias current is particularly important for CBJJ to detect microwave weak signals. Too small a bias current requires a strong external signal to make the JJ be switched into the finite voltage state, and thus it is more difficult to detect the weak microwave signal. On the other hand, however, if the bias current is too large, the existing noise (rather than the signal) makes the JJ be directly switched into its finite voltage state, yielding the detection of the external input signal is fail. To look for the optimal bias current of the CBJJ for the sensitive detection of significantly weak microwave signal, we must make the relationship between the bias current i_b and switching probability by measuring the switched time of the CBJJ. This can be performed as follows. First, solving the Eq. (7) under a certain given bias current, the switching time could be defined as the duration of the phase is evolved from the value $\varphi(0)$ to the time when $\varphi(\tau) > \varphi^* = \pi$, shown schematically as the red line in Fig. 3, wherein the green and blue lines refer to the condition $\varphi(\tau) > \varphi^* = \pi$ is not satisfied and thus the CBJJ is not switched. Secondly, by repeatedly solving the Eq. (7) with a common current i_b multiple times for the random initial phase

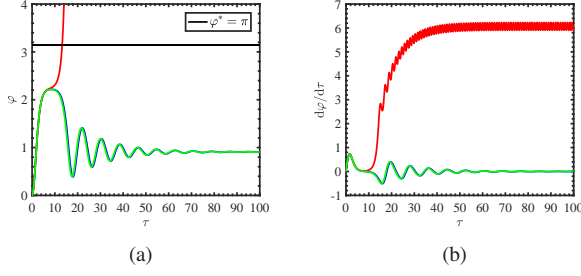


FIG. 3: The simulated phase dynamics (a) and voltage changes (b), by numerically solving Eq. (7). Here, the length of the time step is set as $\delta t = 0.0001$ and the JJ parameters are set as [45]; $I_0 = 8.586 \mu\text{A}$, $R = 29 \Omega$, and $C = 2700 \text{ fF}$, respectively. The biased current is set as $i_b = 0.789$.

$\varphi_i(0)$, $i = 1, 2, \dots$, we get the switching times $P(n)$; Finally, we scan the bias current i_b from 0 to 1 and then find the relationship between the applied bias current i_b and the switching times $P(n)$. From the simulated result shown in Fig. 4(a), one

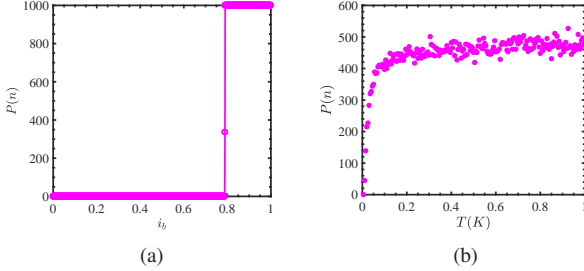


FIG. 4: The numerical simulation of the voltage-state switching of the CBJJ; (a) versus the normalized biased current i_b at $T = 50 \text{ mK}$, and (b) change with the temperature $T(K)$ for $i_b = 0.789$, respectively. Here, $P(n)$ refers to the switching times among the 1000-times simulations. The time step and junction parameters are set as $\delta t = 0.0001$, $I_0 = 8.586 \mu\text{A}$, $R = 29 \Omega$, and $C = 2700 \text{ fF}$, respectively.

can see that, for the fixed background temperature, the switching times $P(n)$ are obviously related to the bias current; the smaller biased current refer to the fewer times of the CBJJ switches, and the optimal bias current for the CBJJ is estimated at $i_b = 0.789$. Also, for a given bias current, Fig. 4(b) shows that the switching times $P(n)$ of the CBJJ are increased with the increase of the temperature. This indicates that the dark switching count is strongly influenced by the temperature, and thus the lower temperature is the more beneficial to improve the sensitivity of the weak signal detection.

Based on the above simulation of the noise-induced switches, we now investigate how the single-induced switches could be distinguishably detected. Under the signal driving, the phase dynamics for the CBJJ can be described by the following equation,

$$\frac{d^2\varphi}{d\tau^2} + \beta \frac{d\varphi}{d\tau} + \sin(\varphi) = i_b + i_n + i_s. \quad (10)$$

According to Eqs. (3) and (4), we know that the applied signal makes the depth of the potential well for trapping the phase particle become shallow, yielding the particle more easily escaped out. This implies that the switching time τ , i.e., the time for the phase to be evolved from $\varphi(0)$ into the value $\varphi(\tau) > \varphi^* = \pi$, might be lowered. Therefore, by comparing the difference between the switching time of the phase particle with and without the microwave signal driving, one can achieve the desired weak microwave signal detection. Certainly, the distinguishability of such a difference, i.e., the detection sensitivity is basically determined by the always-on noise. To quantify such a difference, the so-called Kumar Carroll (KC) index [40, 41];

$$d_{\text{KC}} = \frac{|\langle \gamma_0 \rangle - \langle \gamma_1 \rangle|}{\sqrt{\frac{1}{2}(\sigma_{\gamma_0} + \sigma_{\gamma_1})}}, \quad (11)$$

could be used to represent the difference between two statistical distributions obtained of the phase particle with and without the signal driving. Above, γ_0 and γ_1 are the switching times of the phase particle in the CBJJ without and with the microwave signal driving, respectively. In the present work, they are simulated by numerically solving Eq. (7) (without microwave signal) and Eq. (10) (with microwave signal) respectively for N times with the randomly initial phases. Certainly, due to the always-on thermal noise, the switching times τ_k^i , $i = 1, \dots, N$ must reveal certain statistical distributions with the average

$$\langle \gamma_i \rangle = \frac{1}{N} \sum_{k=1}^N \tau_k^i, \quad i = 0, 1, \quad (12)$$

and the standard variance

$$\sigma_{\gamma_i} = \frac{1}{N(N-1)} \sum_{k=1}^N (\tau_k^i - \langle \gamma_i \rangle)^2, \quad i = 0, 1. \quad (13)$$

for the measurements of N times. Certainly, the larger the value of d_{KC} refers to the higher distinguishability between the two statistical distributions.

With the typical JJ parameters [45]: $I_0 = 8.586 \mu\text{A}$, $R = 29 \Omega$, $C = 2700 \text{ fF}$, we repeatedly solve the Eq. (10) for 1000 times and get the statistical distribution shown in Fig. 5, of the switching times, for different microwave drivings. Accordingly, the relevant KC indexes can be calculated to measure the distinguishing abilities between the statistical distributions with microwave drivings and those obtained for pure thermal noise. Specifically, one can see that if the amplitude of the applied microwave driving is sufficiently large, typically such as $I_{\text{MW}} = 0.001 I_0$, the statistical distribution for the switching times caused by the microwave driving is reliably distinguished from that without the driving, i.e., $d_{\text{KC}} = 2.26 > 1$. An open question is, how weak the microwave signal causes the statistical distribution of the switching times can be distinguished from those purely due to the background noise. Certainly, $d_{\text{KC}} > 1$ refers to the reliable discrimination [57], but it does not mean that two distributions must be indistinguish-

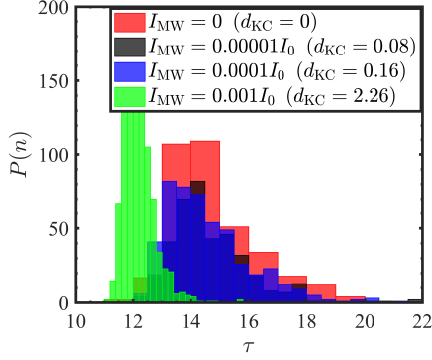


FIG. 5: Simulation of the voltage-state switching times for the CBJJ driven by the different continuous wave microwave currents I_{MW} . Here, the length of the time step is set as $\delta t = 0.0001$ and the parameters CBJJ are set as [45]; $I_0 = 8.586 \mu\text{A}$, $R = 29 \Omega$ and $C = 2700 \text{ fF}$, respectively. Also, the bias current, system temperature, and microwave signal frequency are set as: $i_b = 0.789$, $T = 50 \text{ mK}$, and $\omega_s/2\pi \approx 12.25 \text{ GHz}$, respectively. The d_{KC} indexes of the statistical distribution of the switching events, compared to those with I_{MW} are calculated as $d_{KC} = 0, 0.08, 0.16$, and 2.26 , respectively.

able for $d_{KC} < 1$. Physically, there must be a minimum KC index (which is usually less than 1), i.e., two distributions are still discriminated, if $d_{KC} > \min[d_{KC}] < 1$. This is because the detectability of an energy signal is basically determined by the noise-equivalent power (NEP) of the detector. On the other hand, $\min[d_{KC}]$ refers to the distinguishing ability of the detectable power in the noise background. Therefore, the following task is to determine the $\min[d_{KC}]$ by measuring the NEP of the detector.

Practically, the NEP of the detector can be calculated as [58]

$$\text{NEP} = \frac{S_v}{S}, \quad (14)$$

where $S_v (\text{V}/\sqrt{\text{Hz}})$ and $S = \Delta V/P_{\text{in}} (\text{V}/\text{W})$ are the noise voltage and the detection sensitivity, respectively. $P_{\text{in}} = I_{MW}^2 R$ is the input signal power, and ΔV is the relevant response voltage. For the present CBJJ device, its NEP can be determined as follows. First, the voltage power spectral density S_{vv} of the device can be obtained by solving the Eq. (7) and shown specifically in Fig. 6(a). Consequently, the noise voltage, typically for the signal of frequency 12.25 GHz , can be calculated as $S_v = \sqrt{S_{vv}} = 1.7179 \times 10^{-7} (\text{V}/\sqrt{\text{Hz}})$. Next, the response voltage ΔV of the device can be determined by comparing the difference of the averaged voltages with and without the signal input. With the relevant numerical simulation shown in Fig. 6(b), we find $\Delta V \approx 0.195 \text{ mV}$ for the input $I_{MW} = 0.005 I_0$. Thirdly, the NEP of the CBJJ detector, with the typical parameters $I_0 = 8.586 \mu\text{A}$, $R = 29 \Omega$, $C = 2700 \text{ fF}$ and $i_b = 0.789$, is calculated as $S = \Delta V/P_{\text{in}} = 3.6485 \times 10^9 (\text{V}/\text{W})$, $\text{NEP} = 4.7085 \times 10^{-17} \text{ W}/\sqrt{\text{Hz}}$ for the detection of the signal at the frequency 12.25 GHz . Accordingly, with the NEP

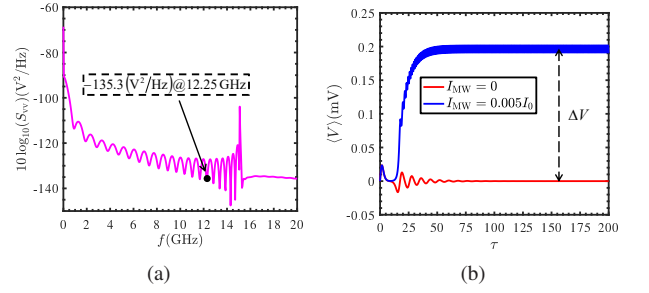


FIG. 6: (a) Numerical results for the thermal noise voltage spectrum of the CBJJ. Here, the length of the time step is set as $\delta t = 0.0001$ and the CBJJ parameters are set as [45]: $I_0 = 8.586 \mu\text{A}$, $R = 29 \Omega$, $C = 2700 \text{ fF}$, and $i_b = 0.789$, respectively. Specifically, at 12.25 GHz , we find that $10 \log_{10}(S_{vv}) = -135.3 (\text{V}^2/\text{Hz})$. (b) Numerical solution to the Eq. (10) for the time-average voltage of the CBJJ, without microwaves (red) and with microwaves driving $I_{MW} = 0.005 I_0$. Here, the normalized bias current of the CBJJ is set as $i_b = 0.789$. The difference between the two voltage averages refers to the responsivity of the CBJJ, i.e., $\Delta V \approx 0.195 \text{ mV}$.

estimated above, the current of the detectable weakest signal is estimated as $I_{\text{min}} = \sqrt{\text{NEP}/R} = 1.2742 \text{ nA}$. In Fig. 7, we simulate the probabilistic distributions of the phase particle escapes with and without the input of the signal current I_{min} . The relevant KC index, i.e., the minimum KC index, is calculated as $\min[d_{KC}] = 0.25$. This means that, with the present CBJJ device, the signals that make $d_{KC} > \min[d_{KC}] = 0.25$ should be detectable.

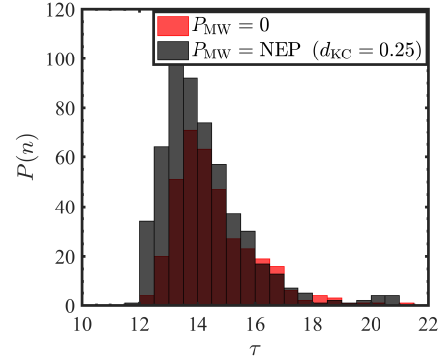


FIG. 7: The simulated statistical distributions of the voltage switching times, by solving Eqs. (7) and (10) for 1000 times, for calculating the NEP-corresponding d_{KC} , i.e., the minimum KC index of the CBJJ. Here, the length of the time step is set as $\delta t = 0.0001$ and the CBJJ parameters are set as [45]: $I_0 = 8.586 \mu\text{A}$, $R = 29 \Omega$, and $C = 2700 \text{ fF}$, respectively. The bias current, background temperature, and microwave signal frequency are set as $i_b = 0.789$, $T = 50 \text{ mK}$ and $\omega_s/2\pi \approx 12.25 \text{ GHz}$, respectively.

III. ESTIMATING THE DETECTABLE MICROWAVE PHOTON NUMBER OF THE CBJJ DETECTOR

In Sec. II, we provided an effective method to simulate the escape events of a driven phase particle in the presence of thermal noise. A minimum KC index $\min[d_{\text{KC}}]$ is introduced to describe the detectability of the signal current along the CBJJ device. Certainly, such a detectability is strongly dependent on the physical parameters of the CBJJ device. Tab. I lists the relevant $\min[d_{\text{KC}}]$ -parameter for the typical CBJJ detectors. Obviously, the lower $\min[d_{\text{KC}}]$ -parameter refers to the lower

TABLE I: The calculated $\min[d_{\text{KC}}]$ indexes for different CBJJs [45, 59, 60] under the best bias current and resonance frequency point. Here, the time step and critical phase are set as $\delta t = 0.0001$ and $\varphi^* = \pi$, respectively.

	JJ1	JJ2	JJ3
I_0 (μA)	8.586	2	0.975
R (Ω)	29	130	290
C (fF)	2700	630	93
T (mK)	50	48	50
i_b	0.789	0.786	0.825
I_{MW}	$0.005I_0$	$0.005I_0$	$0.005I_0$
$\omega_s/2\pi$ (GHz)	12.25	12.28	21.37
NEP (aW/ $\sqrt{\text{Hz}}$)	47.085	26.848	9.623
$\min[d_{\text{KC}}]$	0.25	0.32	0.17

NEP of the CBJJ detector, and thus the higher sensitivity for the detection of microwave photons.

It is emphasized that, in Sec. II the microwave signal is treated as a coherent continuous-wave signal. Below, we assume that a microwave current pulse [61]

$$I_{\text{ph}}(\omega_{\text{ph}}, t_{\text{ph}}, t) = \sqrt{N} \sqrt{\frac{\hbar\omega_{\text{ph}}}{Rt_{\text{ph}}}} \exp\left(-\frac{1}{2}\left(\frac{t-t_d}{t_{\text{ph}}}\right)^2\right) \times \cos(\omega_{\text{ph}}(t-t_d)). \quad (15)$$

with N , ω_{ph} , t_{ph} and t_d being respectively its containing number of photons, frequency, width, and arrival time, etc., flow through the CBJJ detector with the resistance R . The shapes of these pulses through the above three CBJJs are shown schematically in Fig. 8. For these cases, the dynamics for the phase particles of the CBJJ devices should be changed as

$$\frac{d^2\varphi}{d\tau^2} + \beta \frac{d\varphi}{d\tau} + \sin(\varphi) = i_b + i_n + i_{\text{ph}}(\omega'_{\text{ph}}, \tau_{\text{ph}}, \tau). \quad (16)$$

from Eq. (15), where the dimensionless pulse current, microwave frequency, and pulse width are respectively normalized to the critical current I_0 and the Plasma frequency ω_J of the CBJJ, i.e., $i_{\text{ph}} = I_{\text{ph}}/I_0$, $\omega'_{\text{ph}} = \omega_{\text{ph}}/\omega_J$ and $\tau_{\text{ph}} = t_{\text{ph}}\omega_J$.

For the typical three CBJJs listed in Tab. I, we numerical solve the Eq. (16) to simulate the relevant escape events of the phase particle without and with the pulse driving containing, e.g., 30-microwave photons, respectively. The simulated results are shown specifically in Fig. 9. Given the $\min[d_{\text{KC}}]$ -parameter, similar to the usual NEP one, depends completely on the parameters (i.e., the capacitance C , resistance R , and critical current I_0 of the JJ and the biased current i_b) of the

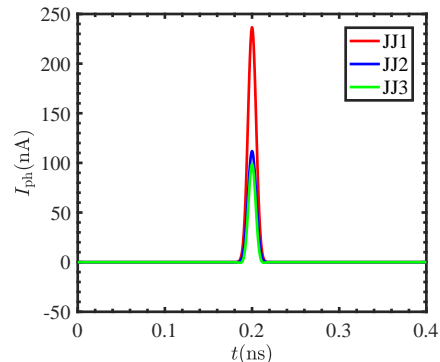


FIG. 8: The shapes of the single-photon microwave current pulses through the three JJs listed in Tab. I with different resistances. The pulse width t_{ph} and arrival time t_d are set as 0.005 ns and 0.02 ns, respectively.

CBJJ device, the detectability of the applied microwave current pulse is thus dependent of if the measured d_{KC} is larger than the corresponding $\min[d_{\text{KC}}]$ -parameter, or not. Therefore, the simulated results shown in Fig. 9 indicate that the applied microwave current pulse of the frequency $\omega_{\text{ph}} = 12.25$ GHz and containing 30-photons, should not be detected by the JJ1-device, as the measured value ($d_{\text{KC}}=0.06$) is manifestly less than its $\min[d_{\text{KC}}]$ -parameter value 0.25. While such a microwave current pulse could be detected respectively by using the JJ2- and JJ3 devices, as the measured values of the d_{KC} indexes (i.e., 1.15 and 1.21, shown respectively in the figure) are manifestly larger than the corresponding $\min[d_{\text{KC}}]$ -parameter values (i.e., 0.25 and 0.17, listed respectively in Tab. I.) This implies that the detectable photon number is basically determined by the $\min[d_{\text{KC}}]$ -parameter of the CBJJ detector. In Tab. II, we list the minimum number of the detectable microwave photons of the frequency 12.25 by using the CBJJ detectors listed in Tab. I. Obviously, the detector with the lower

TABLE II: The calculated $\min[d_{\text{KC}}]$ indexes and detectable photons N for different CBJJs [45, 59, 60] under the best bias current and resonance frequency point. The time step is $\delta t = 0.0001$.

	JJ1	JJ2	JJ3
i_b	0.789	0.786	0.825
$\min[d_{\text{KC}}]$	0.25	0.32	0.17
N	104	24	21

minimum d_{KC} -index possesses the higher detection sensitivity. Given the resistance, capacitance and critical current of the Josephson junction are uncontrollable (once it was fabricated), increasing the bias current seems to be the only effective approach to enhance the detection sensitivity of the CBJJ detector. Based on this idea, in Fig. 10 we numerically predict how the minimum number of microwave photons can be detected by using the JJs listed in Tab. I by optimizing the relevant bias current for the resonant detection of the microwave photons. Here, the frequency of the applied microwave photon is $\omega_s \cong \omega_J^* = (1 - i_b^2)^{1/4} \omega_J$. It is seen that the minimum detectable number of the resonant photons by using the JJ1

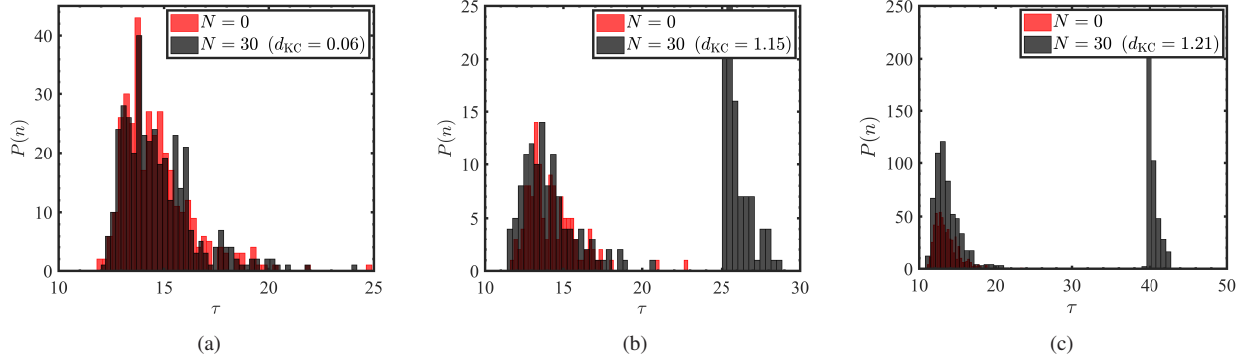


FIG. 9: Numerical simulation results for the voltage state switching times and the corresponding KC-indices for the JJ1 (a), JJ2 (b), and JJ3 (c), driven by the microwave pulses with $N = 0, 30$ -photons. They are obtained by solving Eqs. (7) and (16) for 1000 times, respectively. Here, the time step is set as $\delta t = 0.0001$.

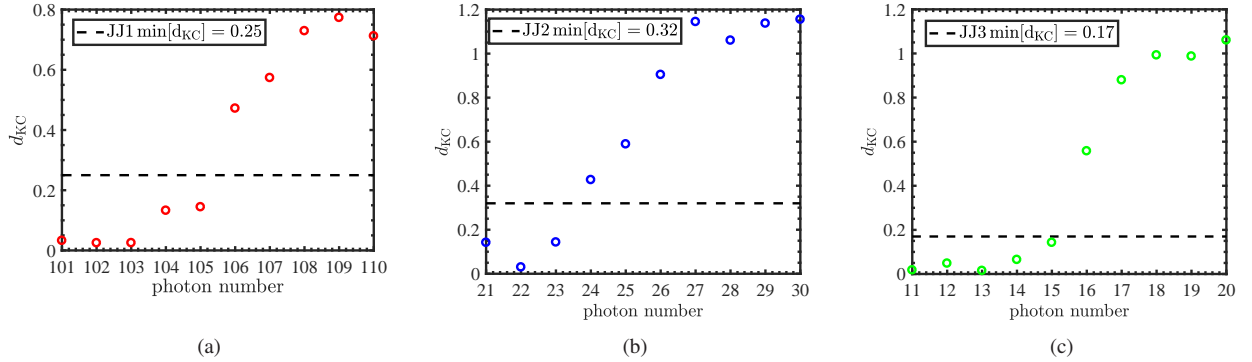


FIG. 10: Numerical predictions of the detectable minimum number of the microwave photons, with the three JJs listed in Tab. I. Here, the time step is set again as $\delta t = 0.0001$. It is seen that the minimum number of microwave photons by using the JJ1, JJ2, and JJ3 are 106 (a), 24 (b), and 16 (c), respectively.

device, with the optimized bias current, is predicted as 106 photons with the frequency being 12.25 GHz; While, the detectable minimum numbers of the resonant photons by using the JJ2- and JJ3 detectors are predicted as 24 at 12.28 GHz and 16 at 21.37 GHz, respectively. They are the approached EQLDs. Probably, to implement the desired EQLD, i.e., the single-photon detection, is required to increase the resistance of the CBJJ and optimize the biased current, e.g., by alternatively using the ac biases.

IV. CONCLUSIONS AND DISCUSSIONS

In summary, by numerically simulating the escaped dynamics for the driven phase particle, we analyzed the detectability of the weak microwave current by using the CBJJ detector. We showed that the difference between the statistical distributions of the probabilistically escaped events of the phase particle, driven by the thermal noises and the applied microwave current, could be quantified by the d_{KC} -index. Physically, the NEP of a detector refers to its $\min[d_{KC}]$ -index. Therefore, if the measured d_{KC} -index is larger than the $\min[d_{KC}]$ -index

of the detector, the applied microwave current signal is detectable. For the typical CBJJ devices, we have predicted their detectable minimum number of resonant microwave photons, by numerically characterizing the relevant values of the $\min[d_{KC}]$ -index, which practically describes the abilities of the devices to discriminate the weakest signals from the noise background. Thanks to the very low operating temperature of the CBJJ detector, the significantly weak microwave current pulse signals, e.g., lowered to a dozen microwave photons approaching to the quantum limit, are still detectable.

It is worth emphasizing that, in our numerical analysis, the NEPs of the typical CBJJ detectors, refers to the measurable minimum d_{KC} -indexes, were estimated as at $\sim 10^{-18} \text{ W}/\sqrt{\text{Hz}}$ level. Following Ref. [58], however, if the noise voltage S_v is reduced to $0.1 \text{ nV}/\sqrt{\text{Hz}}$ by using the lock-in technique, the NEP of these CBJJ detectors could be boosted to the $10^{-23} \text{ W}/\sqrt{\text{Hz}}$ order of the magnitude. This implies that, besides the various developing quantum measurements [62–64], it is still possible, at least theoretically, to implement the desired QLED of microwave photon by using the optimized CBJJ detector [65].

- [1] D. Layne, Receiver sensitivity and equivalent noise bandwidth, *High Frequency Electronics Magazine* **22**, (2014).
- [2] R. Hadfield, Single-photon detectors for optical quantum information applications, *Nat. Photonics* **3**, 696 (2009).
- [3] C. M. Natarajan, M. G. Tanner, and R. H. Hadfield, Superconducting nanowire single-photon detectors: Physics and applications, *Supercond. Sci. Technol.* **25**, 063001 (2012).
- [4] J. -C. Besse, S. Gasparinetti, M. C. Collodo, T. Walter, P. Kurpiers, M. Pechal, C. Eichler, and A. Wallraff, Single-Shot Quantum Nondemolition Detection of Individual Itinerant Microwave Photons, *Phys. Rev. X* **8**, 021003 (2018).
- [5] Z. Wang, L. Balembois, M. Rančić, E. Billaud, M. Le Dantec, A. Ferrier, P. Goldner, S. Bertaina, T. Chanélière, D. Esteve, D. Vion, P. Bertet, and E. Flurin, Single-electron spin-resonance detection by microwave photon counting, *Nature (London)* **619**, 276 (2023).
- [6] B. G. Oripov, D. S. Rampini, J. Allmaras, M. D. Shaw, S. W. Nam, B. Korzh, and A. N. McCaughan, A superconducting nanowire single-photon camera with 400,000 pixels, *Nature* **622**, 730 (2023).
- [7] L. Balembois, J. Travesedo, L. Pallegoix, A. May, E. Billaud, M. Villiers, D. Esteve, D. Vion, P. Bertet, and E. Flurin, Cyclically Operated Microwave single-photon counter with sensitivity of 10^{-22} W/ $\sqrt{\text{Hz}}$, *Phys. Rev. Appl.* **21**, 014043 (2024).
- [8] W. Guo, X. Liu, Y. Wang, Q. Wei, L. F. Wei, J. Hubmayr, J. Fowler, J. Ullom, L. Vale, M. R. Vissers, and J. Gao, Counting near infrared photons with microwave kinetic inductance detectors, *Appl. Phys. Lett.* **110**, 212601 (2017).
- [9] F. Bruccoleri, E. A. M. Klumperink and B. Nauta, Wide-band CMOS low-noise amplifier exploiting thermal noise canceling, *IEEE J. Solid-State Circuits* **39**, 275 (2004).
- [10] H. Milosiu, F. Oehler, M. Eppel, D. Fruehsorger and T. Thoenes, A 7- μW 2.4-GHz Wake-Up Receiver with -80 dBm Sensitivity and High Co-Channel Interferer Tolerance, 2015 IEEE Topical Conference on Wireless Sensors and Sensor Networks 35 (2015).
- [11] J. P. Pascual, B. Aja, E. Villa, J. V. Terán, L. d. I. Fuente and E. Artal, Performance Assessment of W-Band Radiometers: Direct versus Heterodyne Detections, *Electronics* **10**, 2317 (2021).
- [12] X. X. Chen, S. Y. Li, X. X. Xue, and X. P. Zheng, Weak microwave signal detection based on microwave photonics-enabled single-photon technology, In Asia Communications and Photonics Conference, Optical Society of America (2020).
- [13] J. W. May, G. M. Rebeiz, Design and Characterization of W-Band SiGe RFICs for Passive Millimeter-Wave Imaging, *IEEE Trans. Microw. Theory Tech.* **58**, 1420 (2010).
- [14] L. Zhou, C. -C. Wang, Z. Chen, P. Heydari, A W-band CMOS Receiver Chipset for Millimeter-Wave Radiometer Systems, *IEEE J. Solid-State Circuits* **46**, 378 (2011).
- [15] S. Malotau, M. Babaie, M. Spirito, A Total-Power Radiometer Front End in a 0.25- μm BiCMOS Technology With Low 1/f-Corner, *IEEE J. Solid-State Circuits* **52**, 2556 (2017).
- [16] R. Stassi, M. Cirio and F. Nori, Scalable quantum computer with superconducting circuits in the ultrastrong coupling regime, *npj Quantum Inf.* **6**, 72 (2020).
- [17] J. L. O'Brien, Optical quantum computing, *Science* **318**, 1567 (2007).
- [18] R. T. Huang, X. Geng, X. Y. Wu, G. T. Dai, L. L. Yang, J. S. Liu, and W. Chen, Cryogenic Multiplexing Control Chip for a Superconducting Quantum Processor, *Phys. Rev. Appl.* **18**, 064046 (2022).
- [19] Q. He, P. OuYang, H. Gao, S. He, Y. Li, Y. Wang, Y. Chen, X. Dai, Y. Wang and L. F. Wei, Low-loss superconducting aluminum microwave coplanar waveguide resonators on sapphires for the qubit readouts, *Supercond. Sci. Technol.* **35**, 065017 (2022).
- [20] S. Barzanjeh, S. Guha, C. Weedbrook, D. Vitali, J. H. Shapiro, and S. Pirandola, Microwave Quantum Illumination, *Phys. Rev. Lett.* **114**, 080503 (2015).
- [21] H. Zheng, L. F. Wei, H. Wen, and F. Y. Li, Electromagnetic response of gravitational waves passing through an alternating magnetic field: A scheme to probe high-frequency gravitational waves, *Phys. Rev. D* **98**, 064028 (2018).
- [22] A. Berlin, D. Blas, R. T. D'Agnolo, S. A. R. Ellis, R. Harnik, Y. Kahn, and J. Schutte-Engel, Detecting high-frequency gravitational waves with microwave cavities, *Phys. Rev. D* **105**, 116011 (2022).
- [23] L. S. Kuzmin, A. S. Sobolev, C. Gatti, D. Di Gioacchino, N. Crescini, A. Gordeeva, and E. Il'ichev, Single Photon Counter Based on a Josephson Junction at 14 GHz for Searching Galactic Axions, *IEEE Trans. Appl. Supercond.* **28**, 1 (2018).
- [24] T. Braine et al. (ADMX Collaboration), Extended Search for the Invisible Axion with the Axion Dark Matter Experiment, *Phys. Rev. Lett.* **124**, 101303 (2020).
- [25] D. I. Schuster, A. A. Houck, J. A. Schreier, A. Wallraff, J. M. Gambetta, A. Blais, L. Frunzio, J. Majer, B. Johnson, M. H. Devoret, S. M. Girvin and R. J. Schoelkopf, Resolving photon number states in a superconducting circuit, *Nature (London)* **445**, 515 (2007).
- [26] S. Gustavsson, M. Studer, R. Leturcq, T. Ihn, K. Ensslin, D. C. Driscoll, and A. C. Gossard, Frequency-Selective Single-Photon Detection Using a Double Quantum Dot, *Phys. Rev. Lett.* **99**, 206804 (2007).
- [27] W. Khan, P. P. Potts, S. Lehmann, C. Thelander, K. A. Dick, P. Samuelsson and V. F. Maisi, Efficient and continuous microwave photoconversion in hybrid cavity-semiconductor nanowire double quantum dot diodes, *Nat. Commun.* **12**, 5130 (2021).
- [28] M. Esposito, A. Ranadive, L. Planat, N. Roch, Perspective on traveling wave microwave parametric amplifiers, *Appl. Phys. Lett.* **119**, 120501 (2021).
- [29] G. Butseraen, A. Ranadive, N. Aparicio, K. R. Amin, A. Juyal, M. Esposito, K. Watanabe, T. Taniguchi, N. Roch, F. Lefloch and J. Renard, A gate-tunable graphene Josephson parametric amplifier, *Nat. Nanotechnol.* **17**, 1153 (2022).
- [30] A. Mamgain, S. S. Khaire, U. Singhal, I. Ahmad, L. A. Patel, K. D. Helambe, S. Majumder, V. Singh and B. Suri, A Review of Developments in Superconducting Quantum Processors, *J. Indian Inst. Sci.* **103**, 633 (2023).
- [31] J. You and F. Nori, Atomic physics and quantum optics using superconducting circuits, *Nature* **474**, 589 (2011).
- [32] A. I. Braginski, Superconductor Electronics: Status and Outlook, *J. Supercond. Novel Magn.* **32**, 23 (2019).
- [33] G. Romero, J. J. García-Ripoll, and E. Solano, Microwave Photon Detector in Circuit QED, *Phys. Rev. Lett.* **102**, 173602 (2009).
- [34] D. E. McCumber, Effect of ac Impedance on dc Voltage-Current Characteristics of Superconductor Weak-Link Junctions, *J. Appl. Phys.* **39**, 3113 (1968).
- [35] W. C. Stewart, Current-Voltage characteristics of Josephson Junctions, *Appl. Phys. Lett.* **12**, 277 (1968).

- [36] D. V. Anghel, and L. S. Kuzmin, Cold-Electron Bolometer as a 1-cm-Wavelength Photon Counter, *Phys. Rev. Appl.* **13**, 024028 (2020).
- [37] G. Oelsner, C. K. Andersen, M. Reháč, M. Schmelz, S. Anders, M. Grajcar, U. Hübner, K. Mølmer, and E. Il'ichev, Detection of Weak Microwave Fields with an Underdamped Josephson Junction, *Phys. Rev. Appl.* **7**, 014012 (2017).
- [38] E. D. Walsh, D. K. Efetov, G. -H. Lee, M. Heuck, J. Crossno, T. A. Ohki, P. Kim, D. Englund, and K. C. Fong, Graphene-Based Josephson-Junction Single-Photon Detector, *Phys. Rev. Appl.* **8**, 024022 (2017).
- [39] S. Ali, P. H. Ouyang, J. X. He, Y. Q. Chai, and L. F. Wei, Josephson radiation threshold detector, *Sci. Rep.* **14**, 2531 (2024)
- [40] B. V. K. V. Kumar, C. W. Carrol, Performance Of Wigner Distribution Function Based Detection Methods, *Opt. Eng.* **23**, 732 (1984).
- [41] C. Guarcello, A. S. Piedjou Komnang, C. Barone, A. Rettaroli, C. Gatti, S. Pagano, and G. Filatrella, Josephson-Based Scheme for the Detection of Microwave Photons, *Phys. Rev. Appl.* **16** 054015 (2021).
- [42] B. D. Josephson, The discovery of tunneling supercurrents, *Rev. Mod. Phys.* **46**, 251 (1974).
- [43] A. Barone and G. Paterno, *Physics and Applications of the Josephson Effect* (Wiley, New York, 1982).
- [44] E. Ben-Jacob and D. J. Bergman, Thermal noise effects on the microwave-induced steps of a current-driven Josephson junction, *Phys. Rev. A* **29**, 2021 (1984).
- [45] A. L. Pankratov, A. V. Gordeeva, L. S. Revin, D. A. Ladeynov, A. A. Yablokov, and L. S. Kuzmin, Approaching microwave photon sensitivity with Al Josephson junctions, *Beilstein J. Nanotechnol.* **13**, 582 (2022).
- [46] C. M. Falco, W. H. Parker, S. E. Trullinger, and P. K. Hansma, Effect of thermal noise on current-voltage characteristics of Josephson junctions, *Phys. Rev. B* **10**, 1865 (1974).
- [47] R. Menditto, M. Merker, M. Siegel, D. Koelle, R. Kleiner, and E. Goldobin, Evidence of macroscopic quantum tunneling from both wells in a φ Josephson junction, *Phys. Rev. B* **98**, 024509 (2018).
- [48] X. Jehl, P. Payet-Burin, C. Baraduc, R. Calemczuk, and M. Sanquer, Andreev Reflection Enhanced Shot Noise in Mesoscopic SNS Junctions, *Phys. Rev. Lett.* **83**, 1660 (1999).
- [49] C. Guarcello, Lévy noise effects on Josephson junctions, *Chaos, Solitons & Fractals* **153**, 111531 (2021).
- [50] H. Nyquist, Thermal Agitation of Electric Charge in Conductors, *Phys. Rev.* **32**, 110 (1928).
- [51] J. A. Blackburn, M. Cirillo, and N. Grønbech-Jensen, A survey of classical and quantum interpretations of experiments on Josephson junctions at very low temperatures, *Phys. Rep.* **611**, 1 (2016)
- [52] E. L. Wolf, G. B. Arnold, M. A. Gurvitch, and John F. Zasadzinski, *Josephson Junctions: History, Devices, and Applications* (Pan Stanford Publishing, Singapore, 2017).
- [53] R. F. Fox, I. R. Gatland, R. Roy, and G. Vemuri, Fast, accurate algorithm for numerical simulation of exponentially correlated colored noise, *Phys. Rev. A* **38**, 5938 (1988).
- [54] M. Januszewski, M. Kostur, Accelerating numerical solution of stochastic differential equations with CUDA, *Comp. Phys. Commun.* **181**, 183 (2010).
- [55] W. J. Thistleton, J. A. Marsh, K. Nelson and C. Tsallis, Generalized Box-Müller Method for Generating q-Gaussian Random Deviates, *IEEE Trans. Inf. Theory* **53**, 4805 (2007).
- [56] O. V. Pountounigni, R. Yamapi, C. Tchawoua, V. Pierro, and G. Filatrella, Detection of signals in presence of noise through Josephson junction switching currents, *Phys. Rev. E* **101**, 052205 (2020).
- [57] A. S. Piedjou Komnang, C. Guarcello, C. Barone, S. Pagano, and G. Filatrella, Analysis of Josephson Junction Lifetimes for the Detection of Single Photons in a Thermal Noise Background, in 2021 IEEE 14th Workshop on Low Temperature Electronics (WOLTE) (2021), p. 1.
- [58] V. M. Krasnov, Resonant switching current detector based on underdamped Josephson junctions, *Phys. Rev. Appl.* **22**, 024015 (2024).
- [59] A. A. Yablokov, E. I. Glushkov, A. L. Pankratov, A. V. Gordeeva, L. S. Kuzmin, E.V. Il'ichev, Resonant response drives sensitivity of Josephson escape detector, *Chaos Solit. Fractals* **148** 111058 (2021).
- [60] P. H. Ouyang, S. R. He, Y. Z. Wang, Y. Q. Chai, J. X. He, H. Chang, and L. F. Wei, Experimental evidence for a current-biased Josephson junction acting as either a macroscopic boson or fermion, *Phys. Rev. Res.* **6**, 013236 (2024).
- [61] L. S. Revin, D. A. Ladeynov, A. V. Gordeeva, A. L. Pankratov, Response of a Josephson junction to a current pulse with the energy of a microwave photon, *Phys. Solid State* **65**, 1043 (2023).
- [62] Y.-F. Chen, D. Hover, S. Sendelbach, L. Maurer, S. T. Merkel, E. J. Pritchett, F. K. Wilhelm, and R. McDermott, Microwave Photon Counter Based on Josephson Junctions, *Phys. Rev. Lett.* **107**, 217401 (2011).
- [63] A. Poudel, R. McDermott, and M. G. Vavilov, Quantum efficiency of a microwave photon detector based on a current-biased Josephson junction, *Phys. Rev. B* **86**, 174506 (2012).
- [64] A. L. Grimsmo, B. Royer, J. M. Kreikebaum, Y. F. Ye, K. O'Brien, I. Siddiqi, and A. Blais, Quantum Metamaterial for Broadband Detection of Single Microwave Photons, *Phys. Rev. Appl.* **15**, 034074 (2021).
- [65] S. R. He, P. H. Ouyang, H. Y. Gao, Y. F. Li, J. X. He, and L. F. Wei, Nonreciprocity detector arrays for high-efficiency detection of itinerant microwave photons, *Phys. Rev. A* **109**, 062430 (2024).